Electromagnetic cloaking with canonical spiral inclusions

New Journal of Physics
The open-access journal for physics

Electromagnetic cloaking with canonical spiral inclusions

K Guven[1,5], E Saenz[2], R Gonzalo[2], E Ozbay[1,3] and S Tretyakov[4]

[1] Nanotechnology Research Center, Bilkent University, Bilkent 06800, Ankara, Turkey

[2] Electrical and Electronic Engineering Department, Public University of Navarra, Campus Arrosadia, E-31006 Pamplona, Spain

[3] Department of Physics and Department of Electrical and Electronic Engineering, Bilkent University, Bilkent, 06800 Ankara, Turkey

[4] Department of Radio Science and Engineering, Helsinki University of Technology, FI-02015 TKK, Finland

E-mail: guven@fen.bilkent.edu.tr

New Journal of Physics **10** (2008) 115037 (12pp)
Received 13 August 2008
Published 27 November 2008
Online at http://www.njp.org/
doi:10.1088/1367-2630/10/11/115037

Abstract. We report an electromagnetic cloaking structure that is composed of identical canonical spiral particles. By using the Clausius–Mosotti formula, the electric and magnetic polarizabilities of a single spiral particle are related to the relative permittivity and permeability of the sparse distribution of particles. The permittivity and permeability of the distribution are, in turn, defined according to the coordinate transformation, which leads to the cloaking effect. Spirals are optimized to exhibit equal permittivity and permeability response so that the cloak consisting of these spirals will work for both transverse electric (TE) and transverse magnetic (TM) polarizations. Measurement of the cloaking device surrounding a metal cylinder inside a parallel waveguide was performed. The steady-state propagation of an electromagnetic wave was reconstructed from the amplitude and phase data, which demonstrates that the field largely restores to a free-space propagation pattern after the cloak.

[5] Author to whom any correspondence should be addressed.

Contents

1. Introduction

Metamaterials can act as an effective medium with a tailored permittivity or permeability response to an incident electromagnetic wave, which subsequently alters the propagation of electromagnetic waves in unprecedented ways. A recent outcome of this ability was the realization of a conformal mapping medium, which compresses the interior space of a cylindrical region $0 < \rho < a$ into the surrounding cylindrical shell $a < \rho < b$ [1, 2]. The incident electromagnetic waves propagate around the cylindrical region and continue in free space past the cylindrical shell, without any change in phase or amplitude. As a result, an otherwise opaque object that is placed inside the cylindrical region is rendered invisible with respect to the electromagnetic wave. The coordinate transformation is of the form

$$\rho' = \frac{b-a}{b}\rho + a\,; \qquad \varphi' = \varphi\,; \qquad z' = z, \tag{1}$$

which can be implemented effectively by manipulating the material parameters. For the cylindrical cloak, the expressions for the components of the relative permittivity ε_{r} and permeability μ_{r} become [3]

$$\varepsilon_\rho = \mu_\rho = \frac{\rho - a}{\rho}\,; \qquad \varepsilon_\varphi = \mu_\varphi = \frac{\rho}{\rho - a}\,; \qquad \varepsilon_z = \mu_z = \left(\frac{b}{b-a}\right)^2 \frac{\rho - a}{\rho}. \tag{2}$$

All of the corresponding components must be equal and must possess radial dependence, which is a difficult task to realize. The set of relations shown in equation (2) can, however, be simplified so that the ray trajectories inside the cloak remain the same as for the 'full design'. Further simplification is achieved by considering a single polarization for the incident field. For transverse electric (TE) (transverse magnetic (TM)) polarization, it can be shown that a gradient of μ_ρ (ε_ρ) suffices to generate a significant cloaking effect.

The realization of this elegant idea was reported recently for TE polarized waves [3]. The cloak design is based on concentric shells occupying the region $a < \rho < b$, which are decorated with magnetically resonant split ring resonators (SRRs) whose geometrical design parameters are individually determined according to the transformation. Later, a non-magnetic design was proposed theoretically for TM-polarized waves in the optical regime, which is based on radially oriented metallic wires [4].

In the present paper, we design a dual-polarization cloak employing canonical spiral particles [5] and demonstrate the cloaking effect experimentally at microwave frequencies. The

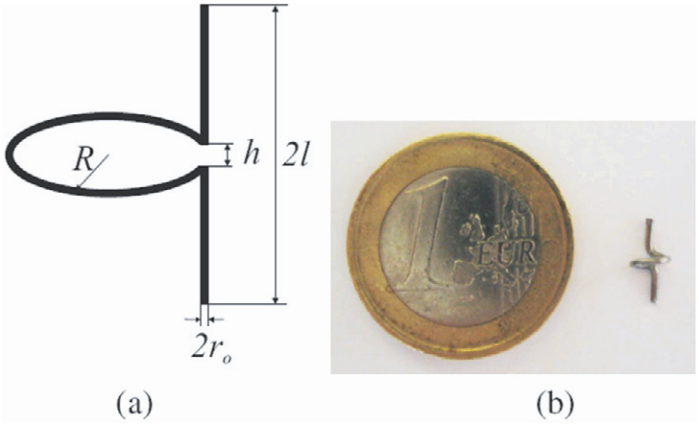

Figure 1. (a) Geometry of the canonical spiral. The relevant parameters are: the radius of the loop, R; the length of the arms, l; the radius of the wire, r_0; and the pitch, h. (b) A photograph of one manufactured spiral.

design is based on the spatial distribution of canonical spirals of the same type, as opposed to employing other resonant particles with different geometrical parameters. By employing canonical spirals with the same dielectric, magnetic and chiral susceptibilities, cloaking can occur for *both* TE and TM polarized incident electromagnetic waves. Moreover, since both electric response and magnetic response are provided by the same particles, it is possible to design a metamaterial with nearly the same frequency dispersion of permittivity and permeability [5], realizing broadband matching. Furthermore, using the same type of resonant particle simplifies the fabrication of cloaks of different sizes. The chirality can simply be compensated for by using a racemic mixture of left- and right-handed spirals in the cloak design [6].

The present paper is organized as follows: section 2 introduces the canonical spiral particles and shows their electric and magnetic responses. In section 3, the design of the cloak is described. The simulated and experimental results of the cloaking device are given in section 4. The last section concludes the paper and provides directions for future work.

2. Canonical spirals

When the cloak is constructed by using spiral particles (see figure 1), the simplified conditions given in [2] can be satisfied for ε and μ simultaneously. The currents induced in a small spiral generate an electric dipole (the wire) and a magnetic dipole (the loop). By adjusting the design parameters (dipole length, $2\,l$, loop radius, R, and the radius of the wire, r_0), the electric and magnetic responses of the particle can be tuned to be identical [6].

Equation (2) can be modified in the following way [5]:

$$\varepsilon_\rho = \mu_\rho = \frac{b}{b-a}\left(\frac{\rho-a}{\rho}\right)^2; \qquad \varepsilon_\varphi = \mu_\varphi = \varepsilon_z = \mu_z = \frac{b}{b-a}. \tag{3}$$

Primarily, we focus on satisfying the condition for the radial parameters $\varepsilon_\rho = \mu_\rho$. The relative permittivity and permeability of a sparse mixture can be approximated using the

Clausius–Mossotti formula (e.g. [6]),

$$\varepsilon_{\mathrm{r}} = 1 + \frac{n}{\varepsilon_0 \,\mathrm{Re}\,\{1/\alpha_{\mathrm{e}}\} - (n/3)}; \qquad \mu_{\mathrm{r}} = 1 + \frac{n}{\mu_0 \,\mathrm{Re}\,\{1/\alpha_{\mathrm{m}}\} - (n/3)}, \tag{4}$$

where α_{e} and α_{m} are the electric and magnetic polarizabilities, respectively, of a single inclusion, and n is the inclusion density per unit volume. By requiring that $\varepsilon_{\mathrm{r}} = \mu_{\mathrm{r}}$, we find that the polarizabilities must satisfy $\alpha_{\mathrm{e}}/\varepsilon_0 = \alpha_{\mathrm{m}}/\mu_0$.

The effective material parameters are implemented by the spiral particle, which consists of an electric dipole and a magnetic dipole (see figure 1). The axial polarizabilities of the spiral are [7,8]

$$\begin{aligned} \alpha_{\mathrm{e}} &= \left[\frac{(\sin kl/k) - l\cos kl}{1-\cos kl} - \frac{1-\cos kl}{k\sin kl}\frac{Z_l}{Z_{\mathrm{W}}+Z_{\mathrm{L}}}\right]\frac{4\tan(kl/2)}{jwkZ_{\mathrm{W}}}, \\ \alpha_{\mathrm{m}} &= -2\mu_0\pi R^3\frac{J_1(kR)}{A_0}\left[1+\frac{j}{Y_{\mathrm{L}}+Y_{\mathrm{W}}}\frac{1}{\pi\eta A_0}\right], \end{aligned} \tag{5}$$

where Z_{W} and Z_{L} denote the impedances of the wire and the loop and Y_{W} and Y_{L} denote the admittances of the wire and loop, respectively. These values can be found in [8].

The operational frequency of the cloak should be near the resonant frequency of the spirals. Otherwise, they are weakly excited. By requiring $\mathrm{Re}\{\alpha_{\mathrm{e}}/\varepsilon_0\} = \mathrm{Re}\{\alpha_{\mathrm{m}}/\mu_0\}$ at the resonant frequency, when $\mathrm{Im}\{Y_{\mathrm{W}}\} = -\mathrm{Im}\{Y_{\mathrm{L}}\}$, the optimal dimensions of the spiral can be obtained. The axial and azimuthal components $\varepsilon_\varphi = \mu_\varphi = \varepsilon_z = \mu_z = b/(b-a)$ are all equal and constant. If we assume that the response of the spiral in the transversal plane (the plane of the loop) is much weaker than in the axial plane, the inclusions will not affect very much those components in which the corresponding permittivities and permeabilities are determined by the background material. If we further design the cloak such that $b \gg a$, the values of permittivity and permeability will become close to unity. In that case, air is a suitable background material.

For the selected operation frequency of 8 GHz, the optimum dimensions are $R = 1.95$ mm and $l = 2.85$ mm [9]. The size of the particle is relatively small ($2l/\lambda < 1/6$). Since the particle size defines the ultimate lower limit on the spatial separation between the particles, a smaller size is better, so that a more uniform distribution of resonant particles and consequently a smoother transition of the permittivity and permeability functions can be realized. A picture of a manufactured spiral is shown in figure 1(b).

The real and imaginary parts of $\alpha_{\mathrm{e}}/\varepsilon_0$ calculated for $R = 1.95$ mm and $l = 2.85$ mm are shown in figure 2.

2.1. Reflection and transmission coefficients for E- and H-coupling

The reflection and transmission spectra of the helix were determined by *S*-parameter measurements of a single spiral placed inside two end-to-end joined waveguide adapters and excited by the TE_{10} mode. In the *E*-coupling measurements, the axis of the spiral is parallel to the incident electric field so that the spiral is seen as an electric dipole. The current induced in the loop also causes a magnetic dipole. However, the magnetic field of this induced dipole is now also *y*-directed and it cannot excite a propagating wave in the TE_{10} mode. In the *H*-coupling measurements, the incoming magnetic field penetrates the loop of the spiral, in turn creating a magnetic dipole. In this case, the secondary electric field, which is excited by the current induced in the 'legs' of the dipole, is unable to propagate.

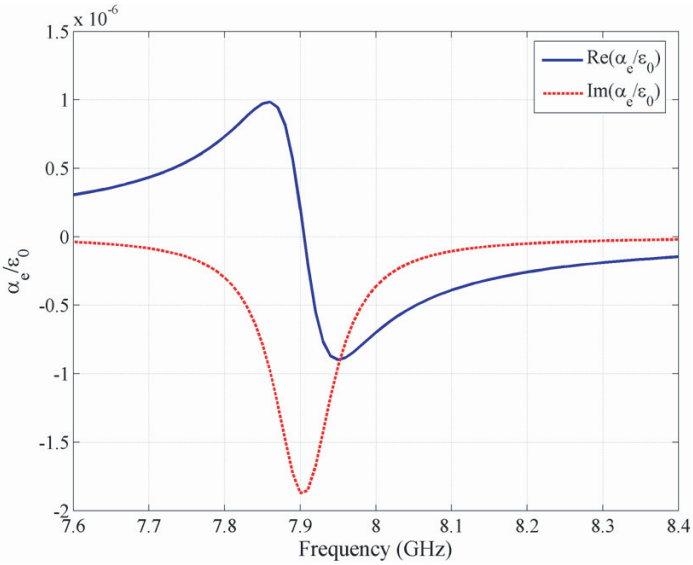

Figure 2. The ratio α_e/ε_0 computed as a function of frequency for the optimum dimensions $R = 1.95$ mm and $l = 2.85$ mm

Right-handed (RH) and left-handed (LH) helices were tested under E- and H-coupling excitations. The results are shown in figure 3. The same resonant frequency ($f \approx 8$ GHz) is obtained for both handednesses and for both polarizations.

3. Cloaking structure

In the proposed cloaking device, the radial alteration of permittivity, ε_ρ, (equation 3) is implemented by changing the inclusion density n as a function of the radial distance ρ, instead of varying the particle sizes as in earlier work [3, 4]. By imposing ε_ρ (equation 3) to be equal to ε_r (equation 4), the density of inclusions as a function of the relative permittivity can be expressed as

$$n = 3\frac{\varepsilon_0}{\alpha_e}\left(\frac{\varepsilon_r - 1}{\varepsilon_r + 2}\right). \tag{6}$$

On the surface of the inner cylinder, $\rho = a$, ε_ρ must go to zero, which means that the value of α_e must be negative and sufficiently large. By choosing α_e/ε_0 close to the resonance ($\alpha_e/\varepsilon_0 = -0.5 \times 10^{-6}\,\mathrm{m}^3$), the density of the inclusions n can be calculated.

The cloak is formed by concentric cylindrical shells that are separated by a distance R_{div} (see figure 4). R_{div} is set equal to 1 cm. For a 3D cylindrical cloak, the layers should be stacked onto each other with an interlayer separation of 1 cm. Taking into account these unit cell dimensions, the number of canonical spirals per row N_ρ can be calculated to satisfy the required spiral density. For a cloak structure in free space, a racemic mixture of canonical spirals is required to compensate for the chirality [9], which means an equal number of RH and LH spirals per unit cell. Therefore, the number of inclusions on each row must be even. When the cloak is placed in a parallel plate waveguide, the chirality is compensated for by mirror imaging from the plates of the waveguide. Hence, only one kind of spiral can be used to construct the cloak for this case.

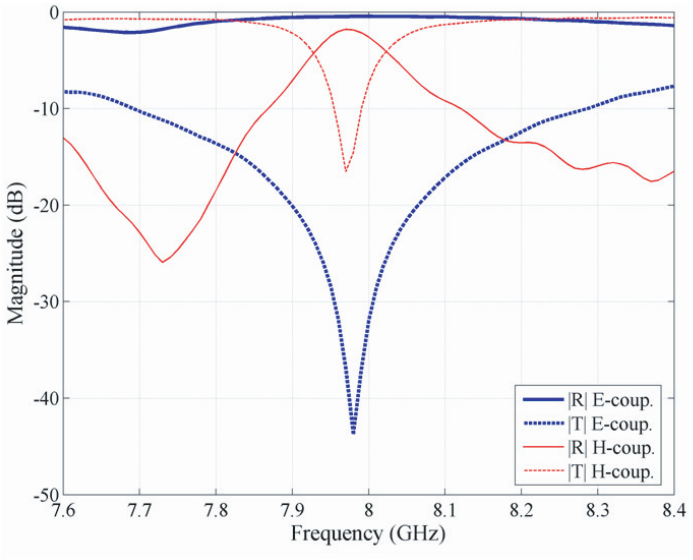

(a)

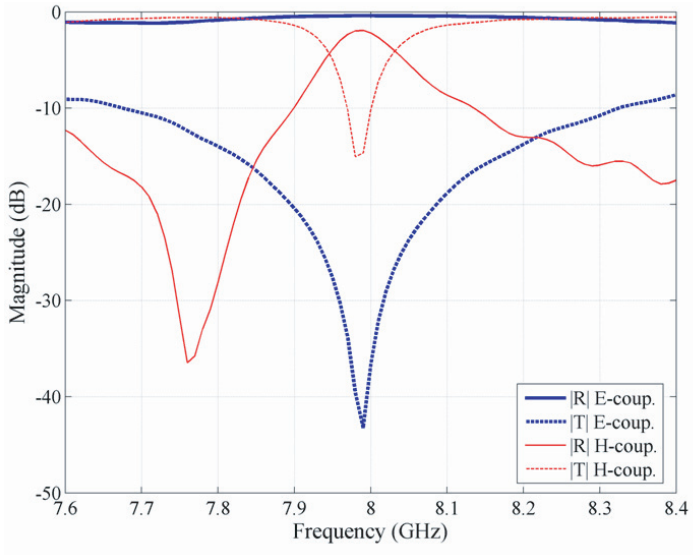

(b)

Figure 3. Reflection and transmission coefficients for *E*- and *H*-coupling. (a) Left-handed helix. (b) Right-handed helix.

The radial distance ρ, permittivity ε_ρ, density of inclusions n, the exact number of spirals per row N_ρ and the even integer number N'_ρ that are used in the design are all shown in table 1. A schematic diagram of the final cloak design is shown in figure 4.

4. Experimental technique

The cloak structure was measured in a 2D parallel-plate waveguide fed with a coax-to-waveguide adapter by the TE mode. The upper plate of the waveguide is patterned by a grid

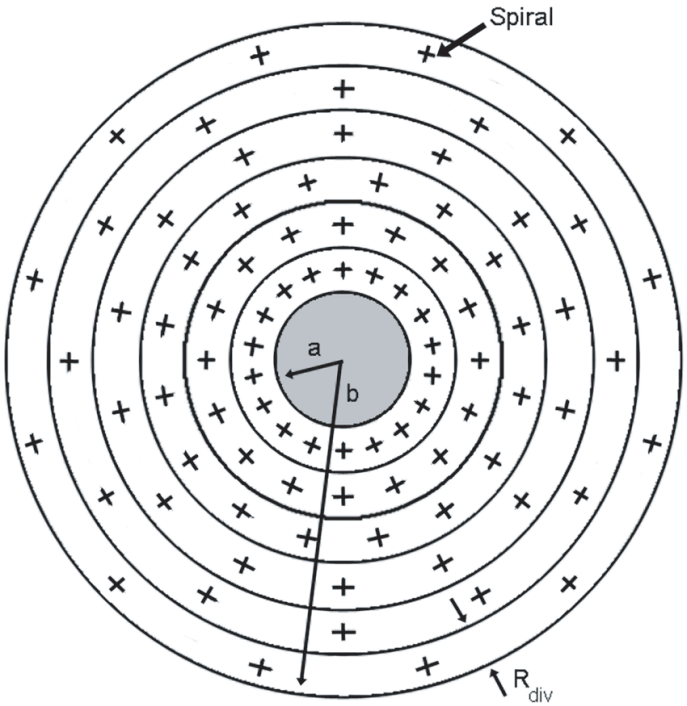

Figure 4. Schematic diagram of the 2D cloak showing the distribution of spirals. The parameters are $a = 1.5$ cm, $b = 7.5$ cm and $R_{\text{div}} = 1.0$ cm.

Table 1. Number of inclusions of the cloak operating at 8 GHz and $\alpha_e/\varepsilon_0 = -0.5 \times 10^{-6}\,\text{m}^3$.

Row	ρ (cm)	ε_ρ	$n(\text{cm}^{-3})$	N_ρ	N'_ρ
1	2	0.08	2.66	16.72	18
2	3	0.31	1.78	16.81	16
3	4	0.49	1.23	15.5	16
4	5	0.61	0.89	13.98	14
5	6	0.70	0.66	12.42	12
6	7	0.77	0.49	10.87	12

of sub-wavelength holes. The radius and lattice constant of the holes were 1.5 and 3.5 mm, respectively. The dimensions were selected such that the plate forms a low-impedance grid and, therefore, it does not disturb the field inside the waveguide. However, the leaky field (around −20 dB) that radiates through the holes can be detected. A monopole antenna that is mounted on a 2D scanning stage detects the real and imaginary parts of the leaky field. The source and detector are connected to an HP8510C network analyzer. The full 2D map of the electromagnetic wave can then be constructed from the measurement data. The edges of the parallel-plate waveguide are isolated by microwave absorbing pads in order to prevent any possible reflection from the open ends. A photograph of the waveguide interior with the top plate of the waveguide in an open position is shown in figure 5.

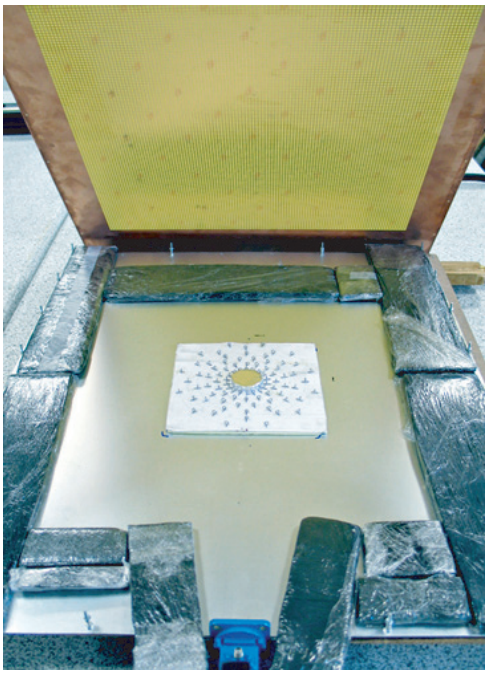

Figure 5. Photograph of the cloak test setup. The upper plate of the parallel-plate waveguide has been opened and is shown to be made of a metallic grid. The cloak is constructed on a white foam pad and then placed in the middle of the waveguide. The sides of the waveguide are covered with microwave absorbers. The coax-to-waveguide adapter feed is shown at the bottom.

The phase of the field is referenced to the output port of the network analyzer. The advancement of the field can be generated by applying an arbitrary phase factor ϕ in $E(x, y)e^{j\phi}$ [10].

First we scan the field of the empty parallel-plate waveguide in order to assess its performance in terms of the propagating mode. The measured real part of the complex electric field at 8.0 GHz is shown in figure 6. Evidently, the propagation does not develop into perfectly planar wavefronts due to the limited distance from the feeding waveguide port, but does manage to provide a good mode profile to investigate the cloaking effect.

The object that is to be cloaked is a metal cylinder that is 3 cm in diameter and 1 cm in height. The bare metal cylinder (marked by the small circle shown in figure 7) is placed in the waveguide and the 2D map of the electromagnetic field is measured. For comparison, we also simulated the experimental structure using a commercial full wave 3D electromagnetic solver. The real part of the measured and simulated electric field is shown in figures 7(a) and (b), respectively. It is worth noting that the experimental field map is constructed from the leaky field 'above' the top plate of the waveguide. This generates the presence of a spurious field above the metal cylinder. In addition, since the incident wavefronts are not perfectly planar, the scattering pattern bears a similar bending. In the simulations, the electric field data are recorded on the bisecting plane *inside* the waveguide. We observe that the measurement and simulation are in good agreement, demonstrating the shadow behind the cylinder due to forward scattering and a standing wave formation between the feeding port and the cylinder due to backward scattering.

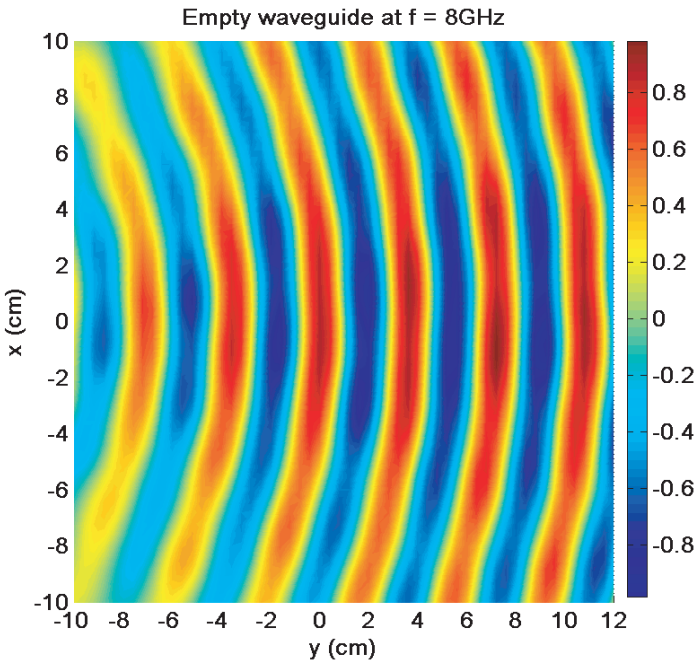

Figure 6. The real part of the electromagnetic field propagating within the empty waveguide at $f = 8$ GHz. The field is fed at $x = 0$ cm and $y = -15$ cm.

Finally, in figure 8, the results for the bare cylinder and the cloaked cylinder are presented. Figures 8(a) and (b) show the electric field amplitude that is computed by commercial numerical software. Again, the field amplitude data are taken on the middle plane inside the waveguide. The localized resonance modes of the canonical spirals are apparent in this simulation. We observe that in the presence of the cloak, the shadow behind the cylinder gets reduced past the cloak boundary where the partial restoration of the electric field is apparent. The backscattering is not completely eliminated either, but this is anticipated due to the approximations made in the design and fabrication of the cloak.

Figures 8(c) and (d) show the measured real part of the electric field for the bare and cloaked cylinders. The spatial resolution of the measurement is affected by the grid spacing of the top plate, which cannot be made arbitrarily small since the amplitude of the leaky field decreases rapidly. The leaky component of the field in the grid holes constructs a 'blurred' view of the actual field profile inside the waveguide. While this may be a drawback against imaging the field around a particular canonical spiral particle, we are mainly interested in the field behavior outside the cloak to investigate backscattering and shadowing. The simulation, however, requires a spatial resolution smaller than the gap of the canonical spirals so that the correct electromagnetic behavior can be generated. With regard to these facts, we stress that the simulation and the experimental plots are intended for qualitative comparison. The experimental result indicates that the wavefronts are starting to restore in the shadow area in the presence of the cloak. Moreover, an encircling behavior of the field around the inner boundary of the cloak can also be observed, which hints at the exclusion of the field from the core region of the cloak. However, the loss inherent to the resonance of the spirals inevitably causes a decrease in transmission amplitude through the cloak. Thus, the overall contrast is reduced in the presence of the cloak.

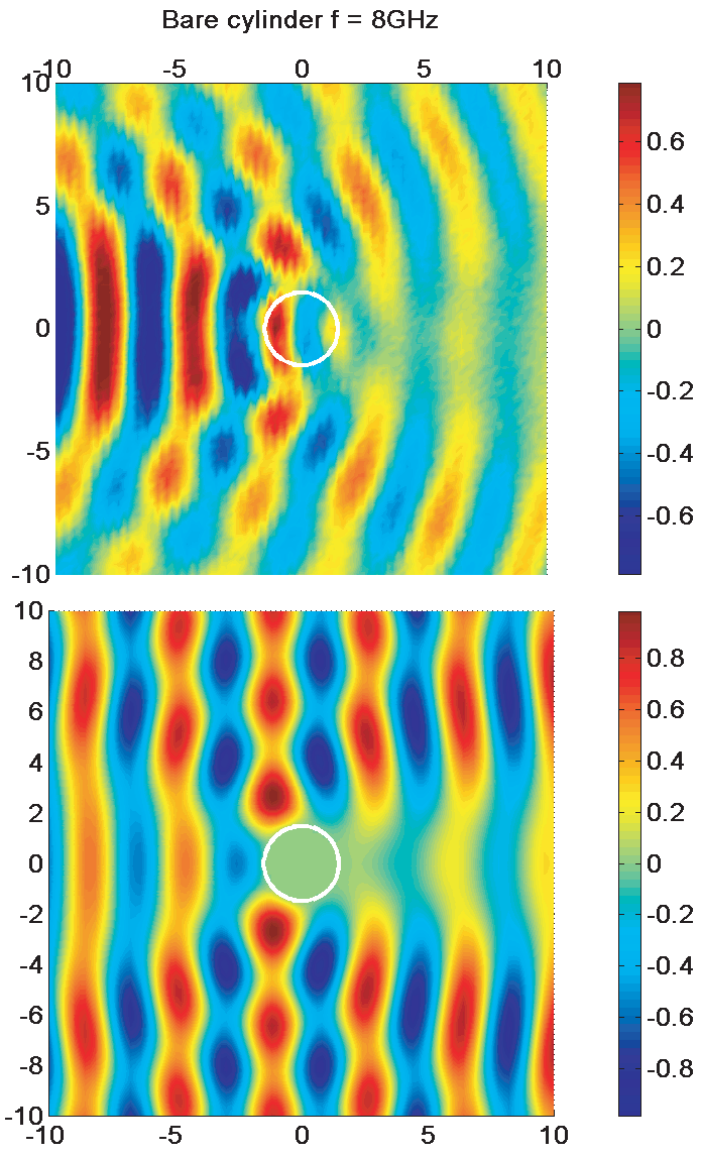

Figure 7. A snapshot of the real part of the measured (top) and simulated (bottom) electric field maps in the presence of the conducting cylinder.

5. Conclusion

In the present work, a cloaking device based on canonical metal spirals is designed and demonstrated experimentally. The required radial alteration of ε in the cloaking device has been obtained by changing the inclusion density of spirals as a function of the radial distance. By using a parallel plate waveguide that incorporated an upper metal grid, images of the propagating field in the presence of the bare metal cylinder and cloaked cylinder were obtained. A comparison of the field images indicates that the cloak manages to reduce the scattering and restoration of the field to the empty-waveguide-mode past the cloak. The cloak design is based on the formulation given by equations (4) and (6). Evidently, the sparse distribution of resonant particles based on the simplified transformation can approximately provide the desired smooth

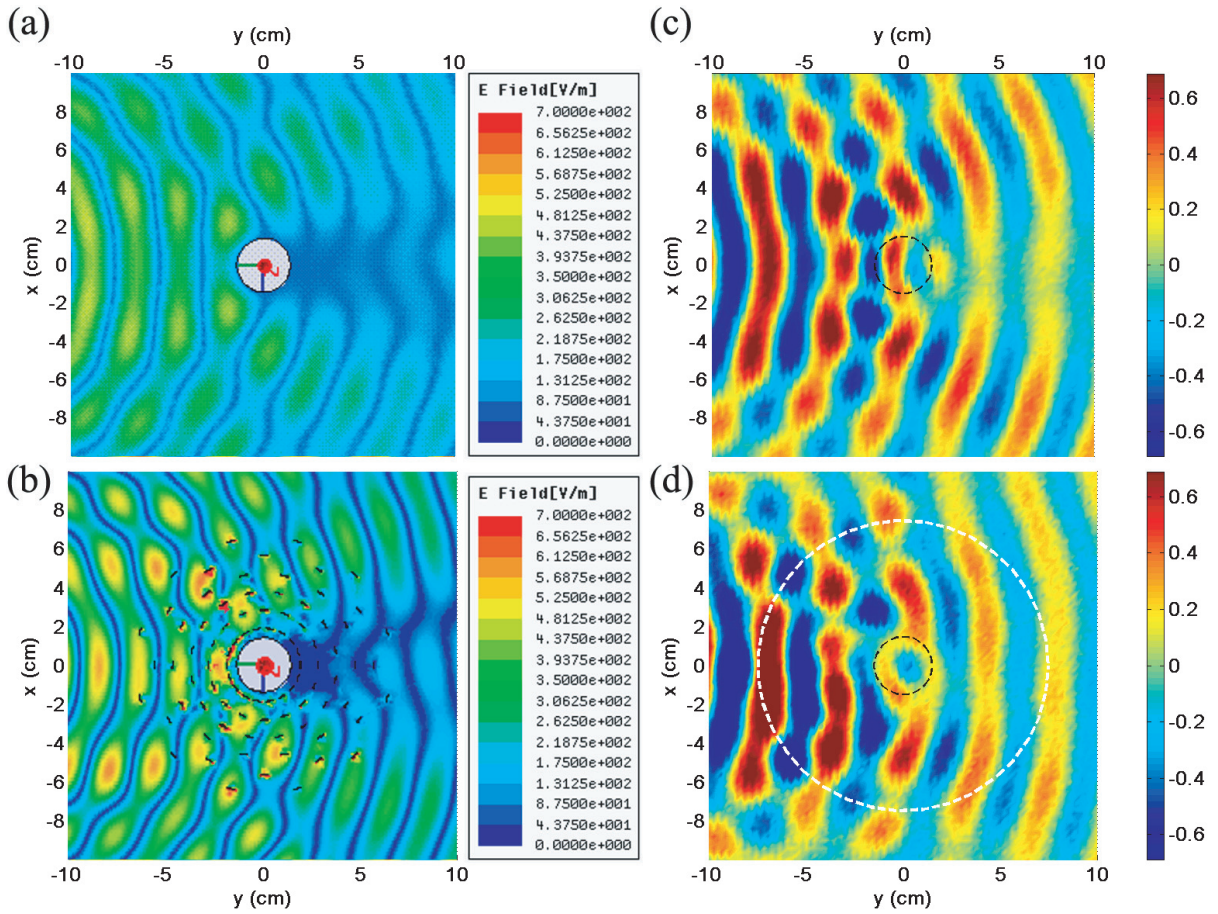

Figure 8. The simulated electric field amplitudes of the (a) bare and (b) cloaked metal cylinders (grey circle). The canonical spirals of the cloak are indicated in black. The measured real part of the electric field of the (c) bare and (d) cloaked metal cylinders. The dashed black line denotes the cylinder location and the dashed white line denotes the outer boundary of the cloak.

transition of the effective parameters. Increasing the particle density can improve the uniformity of distribution provided that the governing transformation equations are still satisfied. On the other hand, by the equality of the permittivity and permeability responses of the canonical spirals, a similar cloaking effect can be obtained for both polarizations. This proof-of-concept design can be applied for larger cloak designs, and for designs that are based on nonlinear coordinate transformations [11].

Acknowledgments

This work was supported by the European Union under the projects EU-METAMORPHOSE, EU-PHOREMOST, EU-PHOME and EU-ECONAM and by TUBITAK under project numbers 105E066, 105A005, 106E198 and 106A017. EO and KG acknowledge partial support from the Turkish Academy of Sciences.

References

[1] Pendry J B, Schurig D and Smith D R 2006 Controlling electromagnetic fields *Science* **312** 1780–2

[2] Leonhardt U 2006 Optical conformal mapping *Science* **312** 1777–80

[3] Schurig D, Mock J J, Justice B J, Cummer S A, Pendry J B, Starr A F and Smith D R 2006 Metamaterial electromagnetic cloak at microwave frequencies *Science* **314** 977–80

[4] Cai W, Chettiar U K, Kildishev A V and Shalaev V M 2007 Optical cloaking with metamaterials *Nat. Photonics* **1** 224–7

[5] Asghar M *et al* 2007 Electromagnetic cloaking with a mixture of spiral inclusions *Proc. Metamaterials' 2007* (*Rome, Italy, 22–24 October 2007*) pp 957

[6] Tretyakov S 2003 *Analytical Modeling in Applied Electromagnetics* (Norwood: MA: Artech House)

[7] Tretyakov S A, Maslovski S and Belov P A 2003 An analytical model of metamaterials based on loaded wire dipoles *IEEE Trans. Antennas Propag.* **51** 2652–9

[8] Tretyakov S A, Mariotte F, Simovski C R, Kharina T G and Heliot J P 1996 Analytical antenna model for chiral scatterers: comparison with numerical and experimental data *IEEE Trans. Antennas Propag.* **44** 106–1014

[9] Saenz E, Semchenko I, Khakhomov S, Guven K, Gonzalo R, Ozbay E and Tretyakov S 2008 Modeling of spirals with equal dielectric, magnetic, and chiral susceptibilities *Electromagnetics* **28** 476–93

[10] Justice B J, Mock J J, Guo L, Degiron A, Schurig D and Smith D R 2006 Spatial mapping of the internal and external electromagnetic fields of negative index metamaterials *Opt. Express* **14** 8694–705

[11] Cai W, Chettiar U K, Kildishev A V, Shalaev V M and Milton G W 2007 Nonmagnetic cloak with minimized scattering *Appl. Phys. Lett.* **91** 111105